Electronic Research Archive

ERA, 32(5): 3113–3129.
DOI: 10.3934/era.2024142
Received: 27 December 2023
Revised: 29 March 2024
Accepted: 12 April 2024
Published: 25 April 2024

http://www.aimspress.com/journal/ERA

Research article

MRI-based model for accurate prediction of P53 gene status in gliomas

Yulin Zhao[1], Fengning Liang[2], Yaru Cao[1], Teng Zhao[1], Lin Wang[1], Jinhui Xu[2] and Hong Zhu[1,2,*]

[1] School of Medical Information and Engineering, Xuzhou Medical University, Xuzhou 221000, China
[2] Department of Computer Science and Engineering, State University of New York at Buffalo, Buffalo 14213, NY, USA

* **Correspondence:** Email: zhuhong@xzhmu.edu.cn; Tel: +8613615105875.

Abstract: The accurate diagnosis and treatment of gliomas depends largely on the understanding of the P53 gene status. In our study, we presented a robust deep learning model, CTD-RegNet (improved RegNet integrating CNN, vision transformer, and truth discovery), tailored for predicting P53 gene status in gliomas. Our model addressed common challenges of existing deep learning models, such as incomplete feature extraction and uncertainty. First, the model used the RegNet network as a basis for predicting P53 gene mutations by skillfully extracting heterogeneous features. Next, the RegNet network was enhanced by integrating the CNN and ViT modules to optimise feature extraction and computational efficiency. Finally, using the truth discovery algorithm, we iteratively refined model uncertainties, thereby improving prediction accuracy. Our experiments demonstrated the effectiveness of the CTD-RegNet model, achieving an impressive accuracy of 95.57% and an AUC score of 0.9789, outperforming existing P53 gene status prediction models. The non-invasive nature of our model minimised the economic burden and physical and psychological stress on patients, while providing critical insights for accurate clinical diagnosis and treatment of gliomas.

Keywords: glioma; P53; deep learning; truth discovery; uncertainty calibration

1. Introduction

Glioma is a type of tumor originating from glial cells, usually occurring in the brain and spinal cord, and is the most common primary malignant tumor [1]. According to the fifth edition of the World Health Organization Classification of Tumors of the Central Nervous System 2021, the role of molecular typing in the diagnosis of gliomas has been further enhanced compared to the fourth edition.

The P53 gene [2] is a critical factor in cell cycle regulation and apoptosis, and it is an important basis for molecular typing of gliomas. Its gene status is divided into wild-type and mutant [3]. Wild-type P53 usually exhibits inhibition of glioma generation, while mutant P53 produces P53 protein with pro-carcinogenic effects after mutation, which inhibits cancer cell apoptosis and aggravates the malignancy of gliomas [4]. Therefore, P53 gene status testing helps in the diagnosis and typing of gliomas, which in turn is of great value in the selection of treatment options, targeted medication, and prognosis. Traditional P53 gene testing for gliomas uses immunohistochemistry or gene sequencing, both of which require invasive puncture biopsy or partial lesion resection for pathological testing to obtain the results. This not only brings risks and irreversible trauma to the patient, but also has an expensive testing cost and a long waiting time. Additionally, the diagnostic results are dependent on the pathologist's experience and professional knowledge to interpret and analyze the results, which may result in subjective diagnostic errors [5].

In recent years, with the development of artificial intelligence technology in the field of medical image processing [6], non-invasive prediction of brain tumor gene status from magnetic resonance imaging (MRI) data has become a research hotspot. Many researchers use imaging genomics to predict the gene status of gliomas. Moon et al. [7] performed imaging genomics feature extraction on multi-parametric magnetic resonance imaging (mpMRI) data, and then implemented a machine learning algorithm with random forests and linear discriminant analysis to predict the expression of P53. Jiang et al. [8] proposed an MRI T2WI-based imaging histology model to predict the P53 gene status in gliomas. One commonly encountered issue by such image-omics methods is that they require doctors to first accurately extract lesions and then obtain high-throughput glioma image features, which often contain a large number of redundant features. Relying on the rapidly developed deep learning techniques in medical image processing [9], Baihua et al. [10] proposed the use of a convolutional neural networks (CNN) model to achieve non-invasive prediction of epidermal growth factor receptor (EGFR) gene status in lung adenocarcinoma. Tatsuki et al. [11] stained P53 cell sections from patients with ulcerative colitis after labeling and annotation, and a CNN model was used to predict P53 gene status. Choi et al. [12] used a CNN model to segment gliomas and then input the segmentation results into a ResNet-34 network to achieve the prediction of isocitrate dehydrogenase 1 (IDH1) mutation status in gliomas. Xu et al. [13] proposed a vision transformer (ViT) framework for multi-tasking gene state prediction for molecular typing of gliomas. Gokhale et al. [14] used a ViT model to achieve the prediction of gene state expression in multiple brain tumors. However, CNNs extract features from image data that are limited to the local area and thus could fail to effectively and comprehensively exploit glioma MR depth image features. The advantage of ViT is that its self-attention mechanism can focus on global features during the image processing task, but tends to ignore local feature extraction. Therefore, further investigation is needed on deep learning models that can pay attention to both local and global features. In addition to the above issues, different network architectures of deep learning models have an important impact on medical image-processing tasks [15]. Since most deep learning models have fixed architectures, the depth and width of the network need to be manually adjusted for different datasets during the training process, which is time-consuming and difficult to accurately capture the heterogeneous features of the data. In addition, deep learning models are perturbed by various factors such as uncertainty inherent in the sample data, uncertainty due to random initialization of parameters, and uncertainty resulting from the use of stochastic gradient descent algorithms during the prediction process, which reduces the accuracy of glioma model prediction [16].

In summary, for the shortcomings of the current deep learning and MR image-based P53 gene

state prediction model for gliomas, such as the inability of the network architecture to adaptively search, the deep heterogeneity of the P53 gene state in glioma images not comprehensively performing feature extraction, and the model being perturbed by a variety of uncertainties, we propose the multimodal P53 gene state noninvasive and accurate prediction model CTD-RegNet, which can not only alleviate the pain and economic burden of patients, but also provide the basis for clinical personalised treatment plans. The specific contributions are as follows:

1) We have adopted the RegNet architecture as the basic model for P53 gene status prediction in gliomas, and adaptively searched and optimally designed the model architecture.

2) Improvement of the model architecture was made using fusion CNN and ViT modules, so that local features and global features participated in the heterogeneous feature extraction of the P53 gene image data; thus, MRI-based glioma P53 gene state prediction was achieved.

3) The truth discovery algorithm was used for iterative optimization to obtain the optimal truth value vectors to calibrate the prediction results, thus obtaining the prediction results with higher confidence and correcting the multiple uncertainties of the model.

2. Materials and methods

2.1. Data collection

The clinical datasets used in this study were collected from local affiliated hospitals and a public dataset, the cancer imaging archive (TCIA). A total of 317 cases (3395 images in total) with MRI data annotated with P53 gene status were collected from the local affiliated hospitals. Ninety of these cases were P53 wild-type patients and the remaining 227 cases were P53 mutant patients. To balance the categories of P53 gene status, the experiment was performed to amplify the data for its wild-type cases, 45 patient images were rotated and 45 were mirrored, and the final number of P53 wild-type cases was 180. Compared with 227 P53 mutant cases, the P53 gene status data were essentially balanced, ensuring the reliability of the experiment. All P53 gene status labels were annotated according to the immunohistochemistry results. The images were all T1c and T2 sequences scanned preoperatively using a 3.0 Tesla machine with the following imaging parameters: repetition time of 2652.94 ms, echo time of 23.28 ms, flip angle of 90°, and resolution of 0.4688 mm. The comparative experiments were performed using the TCIA dataset, which collected MRI data from a total of 208 glioma cases (3416 MR images), of which 91 were P53 mutant type (1604 MR images) and 117 were P53 wild-type (1813 MR images). Data pre-processing includes normalization and resampling of the data. Scaling the pixel values to unify the images to the same scale by the maximum-minimum normalisation method reduced the differences caused by the equipment and scanning parameters; at the same time, in order to eliminate the differences in spatial resolution, the images were resampled to unify the resolution of all the images to the 224 × 224 scale. Meanwhile, this paper quantitatively measured the performance of the proposed method in predicting the P53 gene status of gliomas using five evaluation indices: area under the receiver operating characteristic curve (AUROC), accuracy, precision, recall, and F1-Score. In this paper, the generalization performance of the model and the prevention of overfitting were fully emphasized in all experimental processes, both the affiliated hospital dataset and the public dataset TCIA dataset were divided into the training set and the test set according to the ratio of 8 : 2, and there was no data leakage or data mixing in each experimental session.

2.2. Predicting P53 gene status of gliomas using CT-RegNet

Glioma P53 gene status is crucial for precise diagnosis and treatment. However, accurately capturing the heterogeneous features in many current deep learning networks is challenging, leading to subpar P53 gene status prediction models. Consequently, we have developed a RegNet glioma P53 gene status prediction model that integrates both global and local features. This model aims to effectively extract the heterogeneous characteristics of glioma MRI, thereby enhancing prediction accuracy.

In recent years, neural architecture search (NAS) has been proposed to effectively address the limitations of manually adjusting the model to obtain a high-performance network structure, and can automatically search for the optimal model in the space. However, this method also has certain limitations and is only suitable for searching a single model in a specific domain. Therefore, RegNet [17] leverages the advantages of manual design and NAS to introduce a parametric multi-network 2D design space. The design space constitutes a substantial collection of model systems, and the model architecture is devised by inserting image data into the design space for adaptive exploration, acquiring the optimal width d and depth w, and assessing the model's quality using the error empirical distribution function (EDF) of the analyzed design space. The EDF for models with an error rate of e_p among n models is:

$$F(e) = \frac{1}{n}\sum_{p=1}^{n} 1 \quad [e_p < e], \tag{1}$$

where $F(e)$ is the score of the p model with an error less than e.

(i) First of all, the module width is linearly parameterized:

$$w_j = w_0 + w_a \cdot j \quad \text{for} \quad 0 \le j \le d, \tag{2}$$

where d is the network depth, w_0 $(w_0 > 0)$ is the initial width, w_a $(w_a > 0)$ is the slope, and for each module $j < d$ in the model a different block width w_j is generated.

(ii) Control of w_j change by parameter w_m $(w_m > 0)$:

$$w_j = w_0 \cdot w_{\mathrm{m}}. \tag{3}$$

(iii) The depth d_i of module i is obtained by transforming w_j:

$$d_i = \sum_j 1 \quad [w_j = i]. \tag{4}$$

Random logarithmic uniform sampling is performed within the design space defined by the aforementioned parameters to acquire n models. Subsequently, multiple iterations of sampling are conducted to obtain the optimal width (d) and depth (w), and the high-performance network structure with the lowest error value (error). When compared to the conventional glioma P53 gene state prediction model structure, RegNet can automatically learn the network structure with improved performance and scalability.

The RegNet network architecture is shown in Figure 1.

As shown in Figure 1, the RegNet model has a convolution kernel size of 3 × 3 with a step size of 2. Its body depth comprises d_i blocks that operate at progressively lower resolutions (r_i) for optimal architecture search.

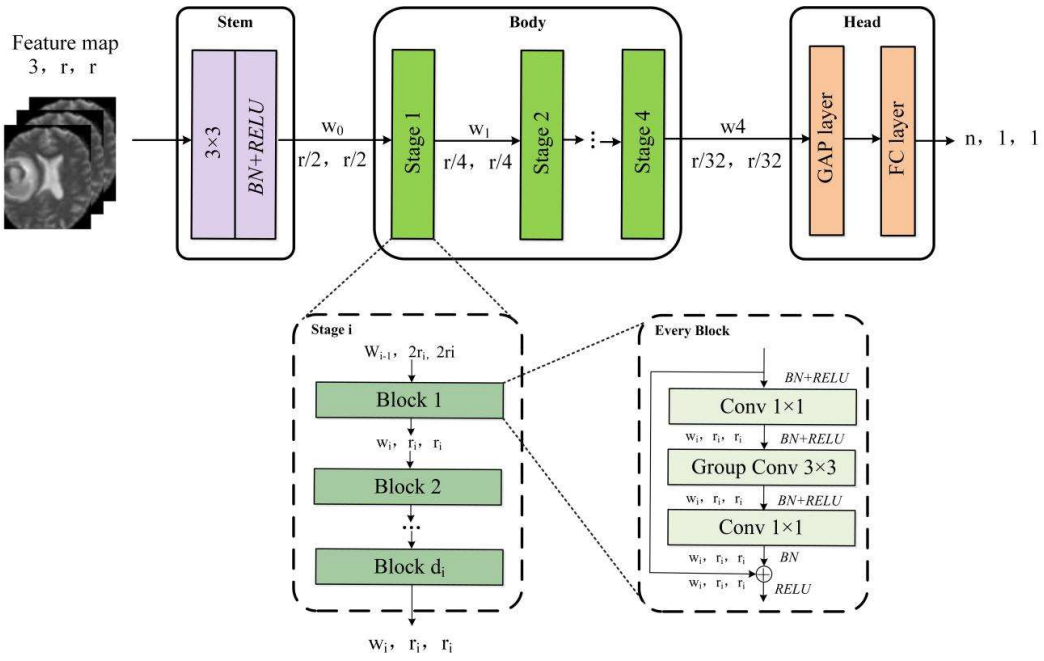

Figure 1. RegNet network architecture diagram.

RegNet can design the optimal network architecture through adaptive searches of parameters within the design space, utilizing input image data. However, the network architecture resulting from RegNet's adaptive search is generated through random logarithmic sampling iterations, introducing a significant degree of uncertainty. Additionally, convolution operations are restricted to local feature extraction, thereby lacking comprehensive learning of image features and potentially compromising model accuracy.

Consequently, CT-RegNet—which integrates both CNN and ViT modules—was developed for glioma MRI feature extraction, aiming to enhance the RegNet network infrastructure by considering both local and global features. This enhancement enables RegNet to extract features more comprehensively, thereby optimizing prediction accuracy for glioma P53 gene mutation status.

Initially, T1c and T2 sequences from glioma MR image data were utilized as inputs for the RegNet network. The embedding block implementation facilitated the extraction of both local and global features from these images, while parameter values for the model group were determined through RegNet's adaptive search within the design space.

The embedding module consists of a CNN block and a ViT block, where the CNN block has a 3 × 3 convolutional kernel consistent with the RegNet convolutional kernel. First, the CNN module is used in the encoder to extract features, which consists of three convolutional layers, each of which is connected and downsampled using an average pooling layer of size 2. After obtaining the output of the convolutional layer through CNN, it is reshaped into a 2D block sequence $\{x_p^i \mid i = 1, 2, 3, \ldots, N\}$ for tokenization, which means image chunking. Let the size of each block (patch) be P × P, then the number of image blocks is $N = HW / P^2$, where H × W is the input image size. Afterward, a linear transformation is done on each of the flattened patch vectors to map them to a D-dimensional vector space. In order to preserve the spatial position information between the input patches, the spatial position information of the patches is encoded and the position-encoded vectors are added into the

patch embedding as a way of preserving the position information. The final result is obtained:

$$z_0 = \left[x_{class}; x_p^1 \mathrm{E}; x_p^2 \mathrm{E}; \cdots; x_p^N \mathrm{E}\right] + \mathrm{E}_{pos}, \tag{5}$$

where x_{class} is the classification vector, E is the patch embedding mapping with output size D, and E_{pos} is the position coding vector.

The resulting high-dimensional input vector is passed to the ViT block. The ViT block comprises the multi-head self-attention (MSA) and the position-wise feed-forward network (FFN). The MSA further comprises three parts: multi-head self-attention, skip connection, and layer normalization (LN); the FFN comprises three parts: feed-forward network, skip connection and layer normalization. z_{l-1} refers to the output of the upper layer's output. Hence, the output of each layer is:

$$\mathrm{z_l} = \mathrm{MSA}\left(\mathrm{LN}(\mathrm{z_{l-1}})\right) + \mathrm{z_{l-1}}, \tag{6}$$

$$\mathrm{z_l} = \mathrm{MLP}\left(\mathrm{LN}(\mathrm{z_l})\right) + \mathrm{z_l}, \tag{7}$$

CT-RegNet achieves the learning of local and global features by fusing the embedding blocks of CNN and ViT modules and inputting the extracted specific features of the glioma P53 gene into the Head module of the RegNet model, which can better capture the global relationship and contextual information in the image. Then, it can search for the optimal model architecture, which can achieve the non-invasive gene state prediction. The structure of the CT-RegNet network is shown in Figure 2.

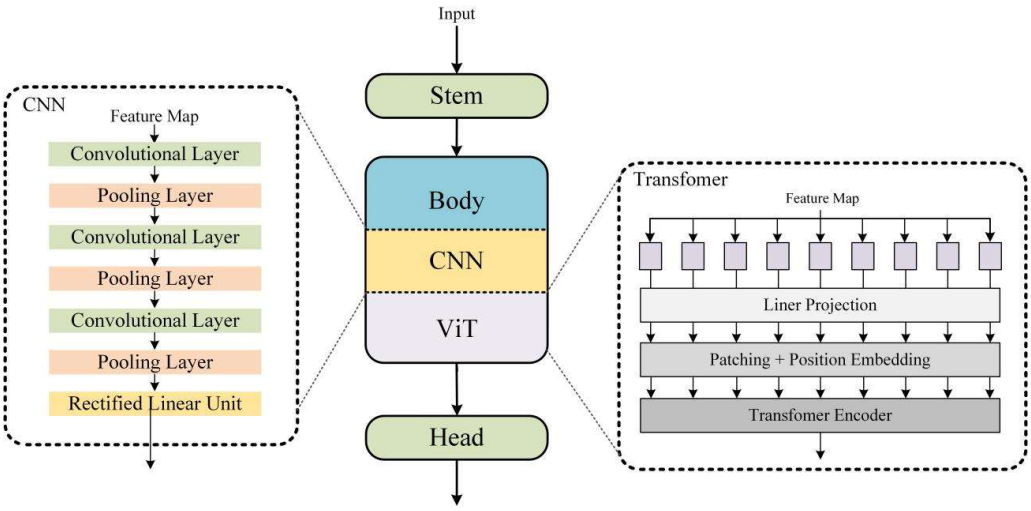

Figure 2. Structure diagram of the CT-RegNet network.

2.3. Accurate prediction model of glioma P53 mutation status based on CTD-RegNet

Although the CT-RegNet model performs well in predicting glioma P53 gene mutation status, it could suffer from various types of uncertainty due to the fact that the parameters of the model group in the network architecture of the RegNet search are generated by iterative random logarithmic sampling. The deep learning model's inherent uncertainty leads to corresponding uncertainty in the high-dimensional vectors' prediction results, and the model's output is affected, leading to incorrect predictions, which impacts medical image classification accuracy. The iterative truth discovery

algorithm can find optimal solutions and gradually improve the accuracy of high-dimensional truth value vectors through multiple iterations, better calibrating the model's uncertainty. Therefore, this algorithm is used to incorporate an improved RegNet network to calibrate uncertainty, resulting in the CTD-RegNet (improved RegNet integrating CNN, vision transformer, and truth discovery) model proposed to enhance glioma P53 gene mutation status prediction accuracy.

The CTD-RegNet model inputs the predicted probability vectors of the CT-RegNet model to the truth discovery algorithm to calibrate the uncertainty of the model. The flowchart of the calibration model for the P53 gene state prediction results based on the truth discovery algorithm is shown in Figure 3.

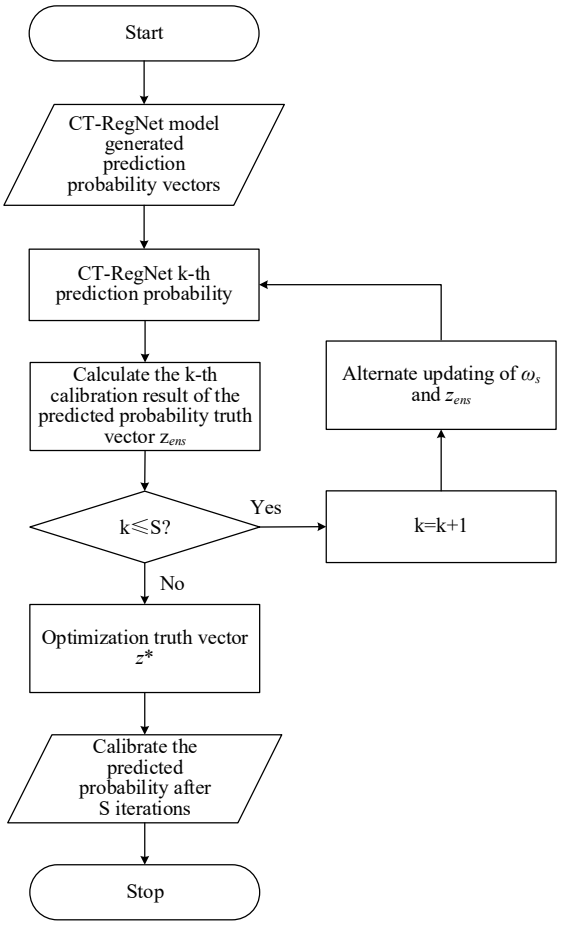

Figure 3. Flowchart of the calibration model of the P53 gene state prediction results based on the true value discovery algorithm.

First, the predicted probability vectors of the P53 gene mutation status of S times glioma produced by the CT-RegNet model under the influence of multiple uncertainties are regarded as S samples for optimal calibration. These are used as $\{z_s\}_{s=1}^{S}$ inputs to the calibration model in the form of high-dimensional P53 gene mutation heterogeneity feature vectors, where $z = f(\theta)$ represents the probability vectors, $f(\theta)$ is the model classifier function, and θ is the classifier prediction weight, whose probability distributions are $q(\theta)$. L represents the number of categories of the input image,

and Δ^L is the probabilistic simplex form in the L-dimensional space, in other words, the prediction result of the model conforms to its distribution in the L-dimensional space:

$$\sum_{l=1}^{L} z_l = 1, 0 \le z_l \le 1. \tag{8}$$

The result of the truth vector integration iteration z_{ens} for the first arbitrary input $x^{(l)}$ is given by Eq (9):

$$z_{ens} = \int f_\theta(x^{(l)}) q(\theta) d\theta. \tag{9}$$

Deep learning models can only handle a finite amount of data, so all data need to be discretized before numerical calculations can be performed. Therefore, the discretization takes the form of Eq (10):

$$z_{ens} = \frac{1}{s} \sum_{s=1}^{S} f_{\theta(s)}(x^{(l)}). \tag{10}$$

Since $z_\theta^{(l)} \in \Delta^L$ and therefore $z_{ens}^{(l)}$ also on the probabilistic simplex, a truth discovery algorithm is used to extract the true probability vector $z^* \in \Delta^L$ for this sample. In addition, the objective function ω_s is used to optimize the confidence of the model and to make the uncertainty of the prediction results converge to a local minimum. The objective function is shown in Eq (11):

$$\begin{aligned} &\min_{z^*, \{\omega_s\}_{s=1}^S} imize \sum_{s=1}^{S} \omega_s \| z^* - z_s \|^2 \\ &s.t. \sum_{s=1}^{S} e^{-\omega_s} = 1. \end{aligned} \tag{11}$$

Let $v_s = e^{-\omega_s}$, therefore, Eq (11) can be converted to:

$$\begin{aligned} &\underset{z^*, \{v_s\}_{s=1}^S}{\text{minimize}} \sum_{s=1}^{S} -\frac{\| z^* - z_s \|^2}{2} \ln v_s \\ &s.t. \sum_{s=1}^{S} v_s = 1. \end{aligned} \tag{12}$$

In the above process, the algorithm looks for the v_s and $\| z - z_{ens} \| /2$ minimization of the cross-entropy of the sum. Where $\| z - z_{ens} \| /2$ is the z_{ens} similarity with each high-dimensional classification vector, i.e., the error between the prediction result and the actual mutation state of the patient; the smaller the error, the more reliable the result. Since the source of uncertainty in the model is unknown, the method of alternatively fixing the truth vector and the confidence level is used to find the optimal confidence level ω_s through Eq (13):

$$\omega_s = \ln\left(\frac{\sum_{i=1}^{S} \| z^* - z_i \|^2}{\| z^* - z_s \|}\right). \tag{13}$$

By updating the truth vector and confidence level in alternating iterations, the uncertainty in the

model prediction results can be converged to a local minimum and the prediction accuracy of the model can be improved. After the confidence level is determined, the truth vector $\sum_{s=1}^{S} \omega_s z_s$ is updated using the predicted probability vector of the CT-RegNet model, and the updated vector remains on the probability simplex. Continuing to update the truth vectors of confidence ω_s and uncertainty $z*$ alternately, the uncertainty of the results is continuously reduced within S iterations of the same sample, and eventually the truth vectors tend to be stable. Then, the iterative updating of the truth vectors and confidence is terminated, and the truth vectors $z*$, whose confidence tends to be aligned with the true probability, are obtained as the predicted probability truth vectors to optimize the results produced in the previous round of iterations. In total, S iterations of calibration are carried out to obtain the prediction results with higher confidence, thus improving the accuracy of the P53 gene mutation status prediction.

The architecture of the entire CTD-RegNet model is shown in Figure 4.

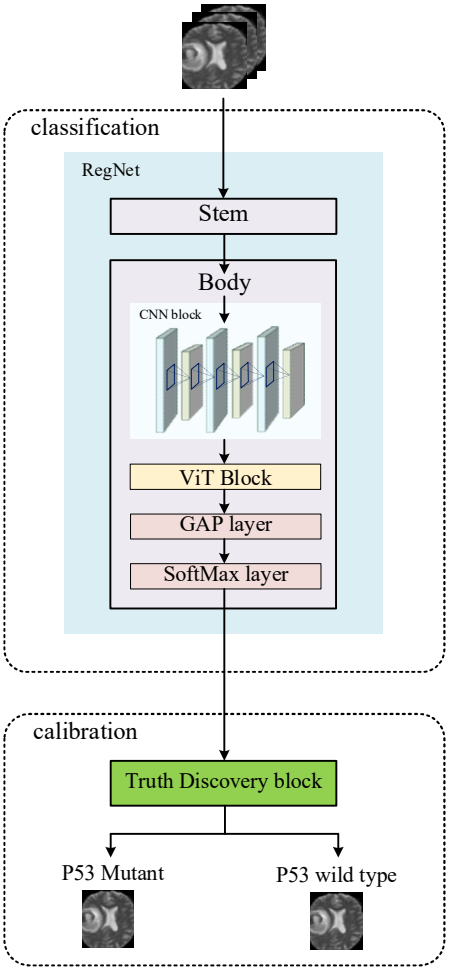

Figure 4. The CTD-RegNet model architecture.

3. Results

3.1. Accurate prediction model of the glioma P53 mutation status based on CTD-RegNet

The glioma MRI data used in this study was fed into the RegNet design space and 500 models

were extracted from the space for 100 rounds of iterative searches to obtain the parameters of the high-performance network structure with the top 10 rankings of minimum error as shown in Table 1.

Table 1. RegNet Optimal structural parameters.

Models	w_0	w_a	w_m	w_j	d_i	Batch size	Error
RegNet-a	24	36.44	2.49	8	13	256	21.1
RegNet-b	24	24.48	2.54	16	22	256	17.3
RegNet-c	48	36.97	2.24	24	16	256	15.9
RegNet-d	56	35.73	2.28	16	16	256	14.8
RegNet-e	80	34.01	2.25	24	18	256	13.0
RegNet-f	88	26.31	2.25	48	25	256	11.7
RegNet-g	96	38.65	2.43	40	23	256	11.4
RegNet-h	184	60.83	2.07	56	17	256	10.8
RegNet-i	80	49.56	2.88	120	23	256	10.3
RegNet-j	**168**	**73.36**	**2.37**	**112**	**19**	**256**	**9.5**

After training, the RegNet-j model had the smallest error rate with a score of 9.5, so the parameters and architecture of this model were selected as the base architecture of the glioma P53 gene state prediction model for feature extraction from glioma MRI data.

3.2. CTD-RegNet-based prediction of P53 gene mutation status in gliomas

In this study, the CTD-RegNet is a novel convolutional neural network designed for predicting glioma P53 gene mutation status. It builds on the foundation of RegNet and incorporates CNN and ViT modules to effectively extract comprehensive local and global features from glioma MRI data. Building on the previous step, the improved RegNet model's uncertainty calibration for glioma P53 gene mutation prediction is conducted using a truth value discovery-based algorithm. This approach effectively mitigates uncertainty errors in the model's predictions while enhancing the confidence level of those predictions. The experimental results demonstrate that the CTD-RegNet network achieves an accuracy of 95.57%.

The results obtained in this experiment for the P53 gene mutation status prediction model in five categorical metrics, such as accuracy, recall, precision, F1-score, and AUC, are shown in Table 2. The experimental results demonstrate that the model proposed in this experiment exhibited superior performance across all metrics, with accuracy, precision, recall, and F1-score reaching 0.9506, 0.9555, 0.9772, and 0.9662, respectively, and the AUC value of the model reaching 0.9789.

Table 2. CTD-RegNet Model test results.

Evaluation indicators	Score
Accuracy	0.9557
Precision	0.9593
Recall	0.9796
F1-score	0.9694
AUC	0.9789

The ROC curve predicted by the CTD-RegNet model is shown in Figure 5.

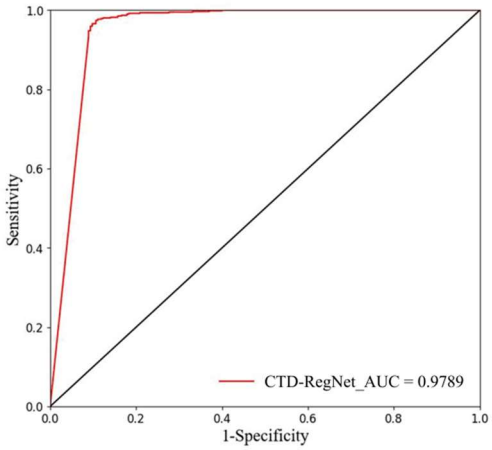

Figure 5. ROC graph of the CTD-RegNet model.

3.3. Ablation experiment

To demonstrate the predictive accuracy and calibration of the proposed CTD-RegNet glioma P53 gene mutation status model, ablation experiments were performed on 317 cases (a total of 3395 MR images) from the affiliated hospitals dataset to demonstrate the robustness and reliability of the model in classification and calibration tasks. The experimental results reveal a notable decrease in accuracy when each module is removed, and it can be concluded that CTD-RegNet, which incorporates the CNN and ViT modules with the truth discovery algorithm, has optimal performance in predicting glioma P53 gene mutation status. The classification accuracy is 85.06% when using only RegNet, 93.88% using the fusion of CNN and ViT modules to enhance RegNet, and 95.57% using the calibrated model incorporating the truth discovery-based algorithm, which is considered to be the model with the highest prediction accuracy that can most accurately predict the glioma P53 gene mutation status. A comparison of model prediction accuracies for ablation experiments is shown in Table 3.

Table 3. Comparison of the results of the ablation experiments.

RegNet	CT block	Truth discovery algorithm	Accuracy (%)
√	√	√	**95.57**
√	√		**93.88**
√			**85.06**

3.4. Comparison of classical models for P53 state prediction results

To validate the prediction accuracy of the proposed CTD-RegNet model, we designed experiments for comparison using the public domain dataset TCIA. The CTD-RegNet model's performance in predicting P53 gene mutation status for gliomas is compared to existing conventional prediction models with various network architectures (Inception-V1, Inception-V2, Inception-V3, ResNet-18, ResNet-34,

and ResNet-50). The results, which also include those using only the CNN model and vision transformer model, are presented in Table 4. The accuracy of the experimental Inception-V1 model is 86.92%, the Inception-V2 model is 85.96%, the Inception-V3 model is 86.85%, the ResNet-18 model is 89.67%, the ResNet-34 model is 88.73%, and the ResNet-50 model achieved an accuracy of 77.93%. The accuracy when using only the conventional CNN model, DesNet121, is 86.90%, and it is 89.20% when using the ViT model. The CTD-RegNet model proposed in this study achieved a prediction accuracy of 94.70%, significantly outperforming the traditional model. The experimental results demonstrate that alterations to internal structural parameters within the same model network can significantly impact the prediction of P53 gene mutation status. Moreover, relying solely on traditional CNN or ViT methods yields unsatisfactory results. Consequently, designing a network structure that facilitates adaptive search while simultaneously integrating CNN and ViT modules plays a crucial role in enhancing both the efficiency and accuracy of the model.

Table 4. Comparison of the P53 state prediction results for the classical model structures.

	Inception Inception V1	Inception V2	Inception V3	ResNet ResNet 18	ResNet 34	ResNet 50	DenseNet 121	ViT	CTD-RegNet (Ours)
Accuracy (%)	86.92	85.96	86.85	89.67	88.73	77.93	86.90	89.20	**94.70**
Precision (%)	92.63	85.22	64.25	44.84	68.19	46.56	90.72	44.60	**94.31**
Recall (%)	88.94	97.58	64.25	50.00	71.37	45.25	76.29	50.00	**98.53**
F1-score (%)	90.74	90.98	64.25	47.28	69.59	45.81	82.88	47.15	**96.38**
AUC	0.9169	0.9139	0.8666	0.5305	0.8329	0.5133	0.8927	0.5355	**0.9657**

In order to verify the superiority of the proposed CTD-RegNet model, we designed comparison experiments with existing MR image-based gene status prediction studies for gliomas in the public domain dataset TCIA, and the results are shown in Table 5. The experimental results show that the prediction accuracy of the CTD-RegNet model proposed in this study is 94.70%, which is significantly better than other existing MR image-based glioma prediction models.

Table 5. Comparison of glioma gene status prediction for existing models.

	Xu et al. [18]	Jiang et al. [19]	Choi et al. [20]	Taha et al. [21]	Kawaguchi et al. [22]	CTD-RegNet (Ours)
Accuracy (%)	93.27	-	78.80	75.00	-	**94.70**
AUC	-	0.8140	0.8600	-	0.8670	**0.9657**

4. Discussion

The CTD-RegNet model uses RegNet as the underlying architecture. RegNet is an efficient image classification network architecture based on convolutional neural networks designed to achieve better performance while keeping the computational cost low. RegNet improves the model performance by individually designing the depth and width of the network to be more scalable and adaptive, and can be applied to various image classification problems. In recent years, deep learning has achieved better

results in the field of medical image processing, but existing MRI-based medical image classification often uses existing network architectures or obtains the height and width of the model through transfer learning and manual adjustment. However, inappropriate depth and width can lead to network performance degradation, resulting in unsatisfactory image heterogeneity feature extraction and affecting the prediction results. The RegNet network can adaptively search the model's width and depth, providing a higher-performance architecture for deep learning models; and the RegNet model adopts a regularized structure to minimize the computation and storage requirements to adaptively design and search for the optimal features, providing the fastest and most efficient network architecture, which can improve the network's robustness and generalization ability, optimize the effect of heterogeneous feature extraction, and improve the model's classification accuracy. A vision transformer (ViT) [23] is the application of a transformer in the field of computer vision. The basic idea of a transformer is to segment an image into fixed-size blocks, and then convert these blocks into sequential data, which can be input into a model for processing. The main advantage of ViT is that it can be used in image processing. The main advantage of ViT is to use a transformer encoder (which mainly contains a multi-layer self-attention mechanism and feed-forward neural network) to extract features from each block in the image to complete the task of image classification or segmentation [24]. ViT is able to capture the global features in an image, which helps improve the performance of image classification and recognition. It is widely used in image classification tasks. However, there are multiple uncertainties in deep learning models, which usually originate from the following aspects: sample data uncertainty caused by unreliable labeling of the acquired data, uncertainty due to random initialization of parameters, and uncertainty arising from the use of stochastic gradient descent algorithms [25]. These uncertainties lead to a decrease in the accuracy of the model's classification results. In turn, the confidence of the model prediction results (i.e., the model's interval estimation of the overall parameters of the sample, which is an index to assess the degree of confidence in the model's prediction) is also affected by uncertainty. Improving model confidence can effectively address the issue of model uncertainty [26]. Label smoothing [27], integrated learning [28], and Bayesian methods [29] are commonly used to calibrate the uncertainty in deep learning models. The truth discovery algorithm [30] aims to find the most accurate observation for each datum from multiple data sources with contradictions or errors [31]. Therefore, in this paper, the truth discovery algorithm is employed to find the optimal value from a large amount of data in which uncertainty is present, thereby reducing the uncertainty of the model. Currently, truth value discovery algorithms are categorized into three types: iteration-based, optimization-based, and probabilistic graphical model-based [32]. In recent years, truth discovery has been widely utilized in the field of medical image processing, encompassing label calibration, model interpretability, performance evaluation, anomaly detection, data enhancement, model calibration, and so on [33]. These applications not only enhance the accuracy, interpretability, and robustness of the medical image processing model but also offer crucial support for the implementation of precision medicine [34].

In this study, we presented an accurate prediction model for predicting P53 gene status in gliomas. First, we used a RegNet network as the basis of the P53 gene mutation status prediction model. The breadth and depth of the model were adaptively designed to help extract different features of the P53 gene. Through the adaptive search of RegNet, the most adaptive model architecture for glioma P53 gene status prediction was finally obtained, so that the infrastructure of this paper can accurately extract the heterogeneous features of the P53 gene. Second, the model integrated the CNN module and the ViT module to design the CT-RegNet model to enhance the ability of the RegNet network to extensively

extract local and global features from MRI data. This integration further optimized the feature extraction capability and computational efficiency of the model, achieving a prediction accuracy of 93.88%. Finally, for the prediction results generated under the presence of multiple uncertainty perturbations in the deep learning model, the truth value discovery algorithm was used for iterative optimization to calibrate the multiple uncertainties in the model results, and the CTD-RegNet model proposed in this paper achieved a prediction accuracy of 95.57%. To verify the effectiveness of the proposed algorithm, we conducted a comparison test with the existing model using the TCIA dataset, and the CTD-RegNet model was the most effective, achieving 94.70% accuracy. In conclusion, CTD-RegNet can accurately predict the P53 gene status of gliomas when dealing with different data sets and high-dimensional prediction vectors with multiple perturbations, and it is more robust than other models, achieving non-invasive and accurate prediction of the P53 gene status, which further enhances the robustness of the model. It also optimizes the predictive accuracy of the model to reduce patient pain and economic burden, and provides more reliable support for accurate clinical use of drugs and diagnostic decision-making by physicians.

5. Conclusions

This paper proposed a CTD-RegNet model for accurate prediction of P53 gene status in gliomas. The model solved the problems of incomplete feature extraction, insufficient model structure, data applicability, and various uncertainty perturbations that lead to reduced prediction accuracy in medical imaging, which are commonly found in current deep learning models. The experimental results showed that the CTD-RegNet model achieved a prediction accuracy of 95.57% for P53 mutation status in the dataset of local affiliated hospitals and 94.70% in the public dataset TCIA. It is demonstrated that the proposed model can achieve non-invasive and accurate prediction of glioma P53 gene status, which improves the prediction accuracy in the existing research field, effectively calibrates the multiple uncertainties existing in the deep learning model, and improves the robustness and generalization of the model. The CTD-RegNet model allows for non-invasive prediction of glioma gene status in clinical practice. This technology is significant in the field of biomedical engineering and provides important benefits to patients and physicians. Specifically, the model greatly improves the patient experience by predicting preoperative genetic status. Compared to traditional invasive testing methods, this non-invasive prediction method is safer and more comfortable, reducing patient trauma on both physical and psychological levels. Additionally, the model provides physicians with important decision-making recommendations to help them develop personalized treatment plans. By predicting the patient's genetic status, doctors can gain a better understanding of the disease's development and the patient's condition. This allows for a more targeted treatment plan, leading to improved therapeutic efficacy and patient survival rates. The CTD-RegNet model also provides valuable preoperative clinical guidance for medical teams, promoting the development of precision medicine and advancing clinical practice. In conclusion, the introduction of the CTD-RegNet model not only improves the treatment experience for patients but also creates new opportunities for future medical research and clinical practice. However, although the CTD-RegNet model has shown promising results in accurately predicting P53 gene status in gliomas, there are some limitations that need to be addressed. Limitations of the study include the potential bias of the dataset used, which may affect the generalizability of the model to different patient populations. In addition, despite the high predictive accuracy, the interpretability and robustness of the models in real clinical settings may be challenging. It is also valuable to continue to

explore the generalizability of the CTD-RegNet model to other tumor types and medical imaging tasks. Adapting the model structure and adopting new techniques may improve performance and applicability in different clinical scenarios. In addition, the integration of more clinical data and additional diagnostic modalities may improve the overall predictive power of the model and its usefulness in clinical practice. By addressing these limitations and exploring new avenues of research, the field of medical imaging and deep learning can be further advanced, and the efficiency of clinical diagnosis and patient care can be improved.

Use of AI tools declaration

The authors declare they have not used artificial intelligence (AI) tools in the creation of this article.

Acknowledgments

The authors are very grateful to the referees for their valuable comments and suggestions, which have helped to improve the paper. This work was supported by the National Natural Science Foundation of China [grant number 62102345], the Project for Research on Medicine of the Jiangsu Commission of Health [grant number Z2020032], and the Xuzhou Key Research and Development Program [grant number KC22117].

Conflict of interest

The authors declare that there are no conflicts of interest.

References

1. P. Sledzińska, M. Bebyn, J. Furtak, A. Koper, K. Koper, Current and promising treatment strategies in glioma, *Rev. Neurosci.*, **34** (2022), 483–516. https://doi.org/10.1515/revneuro-2022-0060
2. Y. Iwatate, I. Hoshino, H. Yokota, F. Ishige, M. Itami, Y. Mori, et al., Radiogenomics for predicting p53 status, PD-L1 expression, and prognosis with machine learning in pancreatic cancer, *Br. J. Cancer*, **123** (2020), 1253–1261. https://doi.org/10.1038/s41416-020-0997-1
3. X. Sun, P. Pang, L. Lou, Q. Feng, Z. Ding, J. Zhou, Radiomic prediction models for the level of Ki-67 and p53 in glioma, *J. Int. Med. Res.*, **48** (2020). https://doi.org/10.1177/0300060520914466
4. I. Ezawa, Y. Sawai, T. Kawase, A. Okabe, S. Tsutsumi, H. Ichikawa, et al., Novel p53 target gene FUCA1 encodes a fucosidase and regulates growth and survival of cancer cells, *Cancer Sci.*, **107** (2016), 734–745. https://doi.org/10.1111/cas.12933
5. D. N. Louis, P. Arie, W. Pieter, D. J. Brat, I. A. Cree, D. Figarella-Branger, et al., The 2021 WHO Classification of Tumors of the Central Nervous System: A summary, *Neuro-Oncol*., **23** (2021), 1231–1251. https://doi.org/10.1093/neuonc/noab106
6. K. Charnpreet, G. Urvashi, Artificial intelligence techniques for cancer detection in medical image processing: A review, *Mater. Today Proc.*, **81** (2023), 806–809. https://doi.org/10.1016/j.matpr.2021.04.241

7. C. M. Moon, Y. Y. Lee, D. Y. Kim, W. Yoon, B. H. Baek, J. H. Park, et al., Preoperative prediction of Ki-67 and p53 status in meningioma using a multiparametric MRI-based clinical-radiomic model, *Front. Oncol.*, **13** (2023), 1138069. https://doi.org/10.3389/fonc.2023.1138069
8. J. J. Jiang, L. M. Guan, Y. Guo, K. Xu, A preliminary study on the predictive efficacy of conventional T_2WI-based radiogenomics model for glioma p53 status, *Chin. J. Clin. Med. Imaging*, **32** (2021), 609–612.
9. I. T. Ashwini, J. T. Senders, S. Kremer, S. Devi, W. B. Gormley, O. Arnaout, et al., Survival prediction of glioblastoma patients-are we there yet? A systematic review of prognostic modeling for glioblastoma and its clinical potential, *Neurosurgical Rev.*, **44** (2020), 2047–2057. https://doi.org/10.1007/s10143-020-01430-z
10. B. Zhang, S. Qi, X. Pan, C. Li, Y. Yao, W. Qian, et al., Deep CNN model using CT radiomics feature mapping recognizes EGFR gene mutation status of lung adenocarcinoma, *Front. Oncol.*, **10** (2021), 598721. https://doi.org/10.3389/fonc.2020.598721
11. T. Noguchi, T. Ando, S. Emoto, H. Nozawa, K. Kawai, K. Sasaki, et al., Artificial intelligence program to predict p53 mutations in ulcerative colitis-associated cancer or dysplasia, *Inflammatory Bowel Dis.*, **28** (2022), 1072–1080. https://doi.org/10.1093/ibd/izab350
12. Y. S. Choi, S. Bae, J. H. Chang, S. G. Kang, S. H. Kim, J. Kim, et al., Fully automated hybrid approach to predict the IDH mutation status of gliomas via deep learning and radiomics, *Neuro-Oncol.*, **23** (2021), 304–313. https://doi.org/10.1093/neuonc/noaa177
13. Q. Xu, Q. Q. Xu, N. Shi, L. N. Dong, H. Zhu, K. Xu, A multitask classification framework based on vision transformer for predicting molecular expressions of glioma, *Eur. J. Radiol.*, **157** (2022), 110560. https://doi.org/10.1016/j.ejrad.2022.110560
14. G. Madhuri, S. M. Kumar, O. Aparajita, GeneViT: Gene vision transformer with improved deepinsight for cancer classification, *Comput. Biol. Med.*, **155** (2023), 106643. https://doi.org/10.1016/j.compbiomed.2023.106643
15. C. Ma, Z. Huang, J. Xian, M. Gao, J. Xu, Improving uncertainty calibration of deep neural networks via truth discovery and geometric optimization, in *Uncertainty in Artificial Intelligence*, PMLR, (2021), 75–85. https://doi.org/10.48550/arXiv.2106.14662
16. L. R. Soenksen, T. Kassis, S. T. Conover, B. Marti-Fuster, J. S. Birkenfeld, J. Tucker-Schwartz, et al., Using deep learning for dermatologist-level detection of suspicious pigmented skin lesions from wide-field images, *Sci. Transl. Med.*, **13** (2021), eabb3652. https://doi.org/10.1126/scitranslmed.abb3652
17. I. Radosavovic, R. P. Kosaraju, R. Girshick, K. He, P. Dollár, Designing network design spaces, in *2020 IEEE/CVF Conference on Computer Vision and Pattern Recognition (CVPR)*, (2020), 10428–10436.
18. Q. Q. Xu, Q. Xu, H. C. Xu, Y. L. Zhao, K. Xu, H. Zhu, Intelligent prediction of glioma IDH1 mutation status based on CnViT, *J. Shandong Univ. Eng. Ed.*, **53** (2023), 127–134.
19. S. Jiang, G. J. Zanazzi, S. Hassanpour, Predicting prognosis and IDH mutation status for patients with lower-grade gliomas using whole slide images, *Sci. Rep.*, **11** (2021), 16849. https://doi.org/s41598-021-95948-x
20. Y. S. Choi, S. Bae, J. H. Chang, S. G. Kang, S. H. Kim, J. Kim, et al., Fully automated hybrid approach to predict the IDH mutation status of gliomas via deep learning and radiomics, *Neuro-Oncol.*, **23** (2020), 304–313. https://doi.org/10.1093/neuonc/noaa177
21. M. B. Taha, M. T. Li, D. Boley, C. C. Chen, J. Sun, Detection of isocitrate dehydrogenase mutated glioblastomas through anomaly detection analytics, *Neurosurgery*, **89** (2021), 323–328. https://doi.org/10.1093/neuros/nyab130

22. R. K. Kawaguchi, M. Takahashi, M. Miyake, M. Kinoshita, S. Takahashi, K. Ichimura, et al., Assessing versatile machine learning models for glioma radiogenomic studies across hospitals, *Cancers*, **13** (2021), 3611. https://doi.org/10.3390/cancers13143611
23. S. Xie, R. Girshick, P. Dollár, Z. Tu, K. He, Aggregated residual transformations for deep neural networks, in *Proceedings of the IEEE Conference on Computer Vision and Pattern Recognition*, (2017), 1492–1500. https://doi.org/10.1109/CVPR.2017.634
24. S. Tummala, S. Kadry, S. A. C. Bukhari, H. T. Rauf, Classification of brain tumor from magnetic resonance imaging using vision transformers ensembling, *Curr. Oncol.*, **29** (2020), 7498–7511. https://doi.org/10.3390/curroncol29100590
25. L. B. Ammar, K. Gasmi, I. B. Ltaifa, ViT-TB: ensemble learning based ViT model for tuberculosis recognition, *Cybern. Syst.*, **55** (2022), 634–653. https://doi.org/10.1080/01969722.2022.2162736
26. C. Guo, G. Pleiss, Y. Sun, K. Q. Weinberger, On calibration of modern neural networks, in *International Conference on Machine Learning*, (2017), 1321–1330. https://doi.org/10.48550/arXiv.1706.04599
27. B. Murugesan, B. Liu, A. Galdran, I. B. Ayed, J. Dolz, Calibrating segmentation networks with margin-based label smoothing, *Med. Image Anal.*, **87** (2023), 102826. https://doi.org/10.1016/j.media.2023.102826
28. T. Buddenkotte, L. E. Sanchez, M. Crispin-Ortuzar, R. Woitek, C. McCague, J. D. Brenton, et al., Calibrating ensembles for scalable uncertainty quantification in deep learning-based medical image segmentation, *Comput. Biol. Med.*, **163** (2023), 107096. https://doi.org/10.1016/j.compbiomed.2023.107096
29. C. Kevin, E. Ralph, Improved calibration of building models using approximate Bayesian calibration and neural networks, *J. Build. Perform. Simul.*, **16** (2023), 291–307. https://doi.org/10.1080/19401493.2022.2137236
30. H. Xu, H. Zhang, Q. Li, T. Qin, Z. Zhang, A data-semantic-conflict-based multi-truth discovery algorithm for a programming site, *Comput. Mater. Continuum.*, **68** (2021), 2681–2691. https://doi.org/10.32604/cmc.2021.016188
31. H. Ding, J. Xu, Learning the truth vector in high dimensions, *J. Comput. Syst. Sci.*, **109** (2020), 78–94. https://doi.org/10.1016/j.jcss.2019.12.002
32. J. J. Cao, C. Chang, N. F. Weng, J. Q. Tao, C. Jiang, Truth value discovery based on neural network coding, *J. Comput. Syst. Sci.*, **43** (2021). https://doi.org/10.3969/j.issn.1007-130X.2021.09.004
33. A. Kumar, P. Liang, T. Ma, Verified uncertainty calibration, *Adv. Neural Inf. Process. Syst.*, **32** (2019). https://doi.org/10.48550/arXiv.1909.10155
34. J. Z. Liu, Z. Lin, S. Padhy, D. Tran, T. Bedrax-Weiss, B. Lakshminarayanan, Simple and principled uncertainty estimation with deterministic deep learning via distance awareness, *Adv. Neural Inf. Process. Syst.*, **33** (2020), 7498–7512. https://doi.org/10.48550/arXiv.2006.10108

AIMS Press